First evidence of widespread active methane seepage in the Southern Ocean, off the sub-Antarctic island of South Georgia

Römer, M.[1,*], Torres, M.[2], Kasten, S.[3], Kuhn, G.[3], Graham, A.G.C.[4,5], Mau, S.[1], Little, C.T.S.[6], Linse, K.[5], Pape, T.[1], Geprägs, P.[1], Fischer, D.[1,3], Wintersteller, P.[1], Marcon, Y.[1], Rethemeyer, J.[7], Bohrmann, G.[1] and shipboard scientific party ANT-XXIX/4

[1] *MARUM – Center for Marine Environmental Sciences and Department of Geosciences, University of Bremen, Klagenfurter Str., 28359 Bremen, Germany*

[2] *College of Oceanic and Atmospheric Sciences, Oregon State University, 104 Ocean Admin Building, Corvallis, Oregon 97331-5503*

[3] *Alfred Wegener Institute, Helmholtz Centre for Polar and Marine Research, Am Handelshafen 12, 27515 Bremerhaven, Germany*

[4] *College of Life and Environmental Sciences, University of Exeter, Rennes Drive, Exeter EX4 4RJ, UK*

[5] *Geological Sciences Division, British Antarctic Survey, High Cross, Madingley Road, Cambridge CB3 0ET, UK*

[6] *School of Earth and Environment, University of Leeds, Leeds LS2 9JT, UK*

[7] *Institute of Geology and Mineralogy, University of Cologne, 50674 Cologne, Germany*

** Corresponding author: Phone +49(0)421 218 65059 Fax +49(0)421 218 65099 E-mail: mroemer@marum.de*

Abstract

An extensive submarine cold-seep area was discovered on the northern shelf of South Georgia during R/V Polarstern cruise ANT-XXIX/4 in spring 2013. Hydroacoustic surveys documented the presence of 133 gas bubble emissions, which were restricted to glacially-formed fjords and troughs. Video-based sea floor observations confirmed the sea floor origin of the gas emissions and spatially related microbial mats. Effective methane transport from these emissions into the hydrosphere was proven by relative enrichments of dissolved methane in near-bottom waters. Stable carbon isotopic signatures pointed to a predominant microbial methane formation, presumably based on high organic matter sedimentation in this region. Although known from many continental margins in the world's oceans, this is the first report of an active area of methane seepage in the Southern Ocean. Our finding of substantial methane emission related to a trough and fjord system, a topographical setting that exists commonly in glacially-affected areas, opens up the possibility that methane seepage is a more widespread phenomenon in polar and sub-polar regions than previously thought.

Keywords: Cold seeps, gas bubble emissions, methane seepage, South Georgia

1. Introduction

As methane is a potent greenhouse gas, considerable research efforts have been made to comprehend its sources and sinks (Intergovernmental Panel on Climate Change (IPCC), 2007). A large part of the methane in the ocean is generated in anoxic marine sediments by methanogens (e.g. Whiticar, 1999; Hinrichs and Boetius, 2002), but sedimentary methane is also formed by thermal breakdown of organic matter occurring at high temperature and pressure. The methane generated in the sediments is influenced by several processes limiting the amount of methane reaching the sediment–water interface. Methane can be removed by hydrate formation in the gas hydrate stability zone (e.g. Hyndman and Davis, 1992). At or near the sediment surface, up to 80% of the

methane is utilized in reduced sediments as a result of the anaerobic oxidation of methane (AOM) (e.g. Barnes and Goldberg, 1976; Knittel and Boetius, 2009). Finally, aerobic methane-oxidizing bacteria at the sediment surface and/or in the water column oxidize methane that has bypassed the anaerobic microbial filter (Hanson and Hanson, 1996; Murrell, 2010). Although the methane flux to the ocean is reduced by these processes, a fraction of methane is injected into the water column. This methane can either be emitted dissolved in fluids or, in case of over-saturation, in form of gas bubbles. Gas bubble emissions are hydroacoustically detectable and are commonly called flares due to their flame-shape appearance in echograms. They often correlate with sub-seafloor anomalies characterized by blanking in the echograms. Such anomalies in the sediment can be caused by upward migrating fluids transporting light hydrocarbons and, thus, may represent gas chimneys fueling the seafloor seepage sites (Judd and Hovland, 1992).

The expanding numbers of seep emission estimates worldwide highlights the importance of methane seepage for the global carbon cycle, and its potential contribution to the oceanic and atmospheric methane inventory, where - in the latter case - methane acts as a potent greenhouse gas. Although the total global atmospheric methane budget is constrained reasonably well (580 Tg yr^{-1}; IPCC, 2007), estimates by source sector vary considerably (Dlugokencky et al., 2011). In particular, global estimations of methane fluxes from geological sources in the marine realm such as natural gas seeps are highly uncertain. At deep-water seep sites most gas bubbles dissolve during ascent through the water column (e.g. McGinnis et al., 2006) and the dissolved methane is further oxidized by microbes (Reeburgh, 2007; Valentine et al.,2001). In contrast, a fraction of gas emitted from shallow water environments may transgress the sea-atmosphere boundary, especially in storm seasons (Shakhova et al., 2013). Therefore, shelf and upper slope areas such as off Spitsbergen (Gentz et al., 2013), in the Black Sea (Greinert et al., 2010), at the Coal Oil Point seep field (Clark et al., 2010; Mau et al., 2012) and off East Siberia (Shakhova et al., 2010) are of particular interest when considering the role of marine methane seepage as possible contributor to atmospheric methane concentrations.

1.1 Marine methane seepage in the Southern Ocean

Sea-floor hydrocarbon seepage occurs at numerous sites on the world's ocean margins, from the continental shelves to the abyssal depths, in a variety of geological settings (Judd and Hovland, 2007; Suess, 2010). Notwithstanding several decades of global methane seep exploration, examples in the Southern Ocean, defined to comprise the water masses south of the Polar Front (Griffiths, 2010), are almost unknown. First videographic evidence of an Antarctic cold seep was obtained by Domack et al. (2005) from the seafloor beneath the collapsed Larsen B ice shelf, western Weddell Sea, located in the trough of the Evans and Crane glacier. This site later was revisited by Niemann et al. (2009), who classified the seepage as inactive, based on the presence of dead shells of seep-associated chemosymbiotic clams (*Calyptogena* sp.), a geochemical sea floor analysis, and the lack of hydroacoustically detectable gas emissions. Apart from this single extinct cold seep site, naturally occurring chemosynthetic organisms (Van Dover et al., 2002) also have been found in the Southern Ocean at hydrothermal vents in the Bransfield Straight (Aquilina et al., 2013; Bohrmann et al., 1999) and the South Sandwich back-arc (Rogers et al., 2012), and at a whale fall from the Kemp Caldera (Amon et al., 2013). The paucity of records of chemosynthesis-based communities in the Southern Oceans can be explained partly by a lack of exploration due to the challenging and remote conditions in this region (Rogers and Linse, 2014). The biogeographic relation to chemosynthetic-based communities at seeps north of the Polar Front, e.g. New Zealand (Davy et al., 2010), offshore Chile (Sellanes et al., 2004) and Australia (Logan et al, 2010), is however largely unknown (Rogers and Linse, 2014).

1.2 Regional setting of South Georgia

South Georgia belongs to the crustal blocks forming the North Scotia Ridge (Fig. 1a), which were once part of the continental connection between South America and the Antarctic Peninsula (Cunningham et al., 1998; Dalziel and Dott, 1975). These crustal blocks were moved during the Cenozoic by backarc spreading and subsequent eastward growth of the Scotia Sea (Cunningham et al., 1998; Forsyth, 1975). There is evidence for active convergence along the western side of the North Scotia Ridge, but

convergence has now ceased along its eastern section, which includes the South Georgia block (Cunningham et al., 1998; Ludwig and Rabinowitz, 1982). However, analyses of an earthquake with its epicenter located south of the South Georgia block (see Fig. 1b) indicates nearly pure thrust faulting, interpreted to represent thrusting of the Scotia Plate beneath South Georgia (Pelayo and Wiens, 1989). This tectonic framework shows that South Georgia is part of an isolated microcontinental block, divided by the W-E trending Cooper Bay Shear Zone that crosses the Island (Fig. 1b). This is the major tectonic boundary that displaces the late Jurassic to early Cretaceous basement complexes exposed on South Georgia (Curtis et al., 2010).

In contrast to the geologic and tectonic evolution of South Georgia, the shelf and upper slope area surrounding the Island have been less well studied. However, a recent comprehensive bathymetric compilation aimed at elucidating the paleo-ice sheet drainage of the island has greatly improved our knowledge of the continental shelf morphology of South Georgia (Graham et al., 2008). These researchers described large eroded troughs linked to the recent fjords around South Georgia (Fig. 1b; for the purpose of this study numbered 1-10), and they proposed that these cross-shelf troughs were formed during glacial times and represent former pathways of outlet glaciers and ice streams. Although probable Mesozoic sedimentary and volcanic rocks extend beneath the inner shelf of South Georgia, Cenozoic sediments form the outer parts of the continental shelf (Graham et al., 2008; Simpson and Griffiths, 1982).

South Georgia is located in the path of the Antarctic Circumpolar Current (ACC). The Polar Front is located to the north and the southern ACC front loops anticyclonically around the island from the south before retroflecting to the east (Thorpe et al., 2002). The shelf waters of South Georgia are often markedly different from the open waters, indicating that local processes are important in dictating shelf water mass characteristics (Young et al., 2011). Various shelf-specific processes have been observed, or inferred at South Georgia, and significant interannual variability of the oceanographic conditions on the shelf are known (Meredith et al., 2005; Young et al., 2011). In general, the special oceanographic conditions around South Georgia result in a rich ecosystem, with

large phytoplankton blooms and related strong atmospheric carbon drawdown (Borrione and Schlitzer, 2013; Jones et al., 2012), as well as high organic matter sedimentation on the shelf. The seasonally occurring blooms are particularly intense on the northern shelf area of South Georgia and within the adjacent Georgia Basin (Borrione and Schlitzer, 2013).

Seepage of methane has not been reported so far near South Georgia. During Polarstern cruise ANT-XXIX/4 we explored the northern shelf of South Georgia to identify any seeps that might originate from the high organic matter load on the continental shelf. We first performed a comprehensive hydroacoustic survey to detect gas seepage, which we subsequently investigated by visual seafloor observation and correlated with methane analysis in the sediments and water column that together extend our understanding of methane-related processes taking place in the local hydrosphere.

2. Methods

2.1 Hydroacoustic systems

The data used for this study were acquired during R/V Polarstern cruise ANT-XXIX/4 in March and April 2013 (Bohrmann, 2013). Bathymetric mapping was performed using an ATLAS Hydrosweep Deep-Sea 320-beam echosounder operating at a frequency of ~15 kHz and covering a swath width about four times the water depth. Raw data were processed with the commercially available hydrographic processing systems CARIS 7.0 HIPS and SIPS and the open source seafloor mapping software MB (MultiBeam)-System (Caress et al., 2012). The grids produced were visualized with the geographic information system ESRI ArcMap 10.0. The cleaned Hydrosweep data were gridded with a cell size of 25 m. We combined our results with additional data from earlier cruises of the British Antarctic Survey (Fretwell et al., 2008) (available at http://www.antarctica.ac.uk/bas_research/data/online_resources/sgbd/) and the GEBCO dataset (http://www.gebco.net/).

We used the ship-mounted parametric single beam echosounder (SBES) ATLAS PARASOUND for shallow subbottom imaging. The secondary low frequency (SLF) of about 4 kHz was recorded and processed online with the software ATLAS PARASTORE. The resulting PS3-files were imported to

SENT (H. Keil, University of Bremen) and the data plotted. In addition, the SBES ATLAS PARASOUND was used for imaging of rising gas bubbles ('flare detection') that show up as backscatter anomalies in echograms using the primary high frequency (PHF) of about 18 kHz (Fig. 2a). The transducer opening angle was 4°, resulting in a footprint size of about 7% of the water depth. PARASOUND data as well as metadata are available at the PANGAEA data repository.

2.2 Seafloor observations

The Ocean Floor Observation System (OFOS), a towed underwater system equipped with a high-resolution digital camera (ISITEC, CANON EOS 1Ds Mark III), was used to visually inspect the sea floor at an altitude of about 1.5 – 2 m relative to the seabed in areas where flares were detected. In addition to the provided live feed, the camera was programmed to take high-resolution (21 megapixels) photographs of the sea floor every 30 seconds. Underwater-navigation was achieved using the shipboard IXSEA Posidonia ultra short baseline system, with an accuracy of 5 – 10 m, and these data were used to establish the OFOS tracks and the positions of each photograph taken.

2.3 Water column analyses

Water column properties were investigated deploying a 24-Niskin water bottle rosette to which a CTD-unit was attached (Seabird, SBE 911+). Using the sensors of the CTD-unit, salinity, temperature, and pressure data were measured. In addition, a Sea-Tech transmissometer and a SBE 43 sensor was used to record beam transmission and concentrations of dissolved oxygen, respectively. For quantification of methane concentrations in the water column, 750 ml of sampled seawater were transferred from the Niskin bottles into pre-evacuated 1000 ml glas bottles immediately after recovery. Gas was extracted from these samples using the modification of the vacuum degassing method described by Rehder et al. (1999). The extracted gas was analyzed onboard with a 6890N gas chromatograph (Agilent Technologies) equipped with a capillary column and connected to a Flame Ionization Detector, as described in Pape et al. (2010). Calibrations and performance checks of the analytical system were conducted regularly using commercial pure methane standards. The coefficient of variation determined for the analytical procedure was less than 2%.

2.4 Stable carbon isotope signatures

Three sediment gas samples were extracted from two gravity cores taken close to flare origins (GC-1: station PS81/280-1 in cross-shelf Trough 6, Fig. 3a; GC-2: station PS81/284-1 in Cumberland Bay, Fig. 3b) were analyzed for stable carbon isotope ratios of methane. The samples were obtained from depths between 6 and 9 meters below sea floor (mbsf), which was below the depth of the sulfate-methane transition (Chapter 9 in Bohrmann, 2013), and therefore should not have been influenced by potential anaerobic methane oxidation. Sediment (3 ml) was sampled from the bottom of each of the freshly cut core sections were taken immediately after core recovery using cut-off syringes and transferred into 20 ml glass vials prefilled with 5 ml of 1 M NaOH. The headspace gas was sampled for onboard methane concentration analyses (Pape et al., 2014) and a subsample was used shortly after arrival at the home laboratory for shore-based measurements of its stable isotope signature. Analysis of stable C isotope signatures of CH_4 was conducted at the commercial GEO-data GmbH laboratory (Garbsen, Germany). Stable C isotope ratios are reported in δ-notation in parts permil (‰), relative to the Vienna PeeDee Belemnite (V-PDB) standard. The reproducibility of stable carbon isotope determinations is estimated at ±0.1‰.

3. Results

3.1 Hydroacoustic observations

Hydroacoustic surveys revealed the presence of numerous gas emission sites at water depths between 130 and 390 meters below sea level (mbsl) on the northern shelf of South Georgia in spring 2013. The gas emissions appeared as ‘flares’ in the echograms due to the high impedance contrast of free gas emanating as bubbles through the water column, which produce a high-backscatter signal (Fig. 2a). The flares were composed of vertically arranged oblique reflections that image the up-rising individual bubbles or groups of bubbles, and make them discernible from fish schools. In total, at least 133 individual flares were detected during our study (Figs. 3a and b, supplementary table S1). The flares showed largely straight and vertical orientation (e.g. the 170-m high ‘Cumberland Bay Flare’, Fig. 4c), indicating a lack of strong currents that would be expected to deflect the bubbles

during their rise through the water column. Roughly 75 % of the flares were less than 100 m high, with an average of ~70 m (supplementary table S1). However, three flares extended from the sea floor to a height of at least 25 mbsl. The uppermost part of the echograms was disturbed by acoustic noise that hampered differentiation of gas bubbles from plankton and/or fish. In general, the real flare height was difficult to determine using Parasound recordings, as the small ~4° opening angle and a coherent narrowing footprint with decreasing depth impeded the detection of the uppermost part of the flares when the ship did not pass exactly through the center of the bubble train.

Many flares detected were discontinuous or were disconnected from the sea floor (Figs. 4a and b). This observation can be attributed to horizontal deflections of a bubble stream that moves in and out of the conical Parasound beam, or to transient gas bubble streams where the emissions are temporally variable. The latter explanation seems to be more likely in this case, as the tall flares appeared vertical and did not show strong lateral deflections; however, variable current regimes cannot be ruled out entirely.

The temporal variability of the flares was examined by imaging a given location more than once. Four flares became visible at the same location two times within ca. 14 days, whereas eight other flares appeared only once, although surveyed twice (supplementary table S2). The observations of the flare appearance and the repeated surveys show that most flares probably are temporally variable on scales of minutes to weeks.

The detected flares were not randomly distributed along the northern South Georgia margin. They occurred either within the Cumberland Bay fjord system or within the other incised cross-shelf troughs that cut through the broad shelf surrounding the island (Fig. 3a). Two fjord systems were inspected for the occurrence of flares during cruise ANT-XXIX/4: Cumberland Bay was investigated intensively (Fig. 3b), whereas Possession Bay was entered once and inspected only along two survey lines. While numerous flares were observed in the Cumberland Bay region, no indication of gas emissions were found in Possession Bay. In total, more than 75 flares were detected in both

branches of Cumberland Bay and within the cross-shelf to which the fjord system connects (designated as Trough 5 in Fig. 3b). Flares were distributed close to the fjord-mouth and within the fjord itself, but were not detected in the innermost parts of the bay close to the glaciers that discharge into the fjord at the coast. A few flares were found within the ~10 km area seaward of the fjord mouth, and one flare was detected as far as ~30 km from land. In addition to cross-shelf Trough 5, gas emissions also were found in four of the seven troughs defined by Graham et al. (2008) on the northern shelf of South Georgia (Fig. 3a). The northern shelf was hydroacoustically surveyed twice in a roughly two week interval, and during both investigations, flares were observed to be restricted to the troughs. No flares were detected on the shallower banks between the cross-shelf troughs and, with the exception of Troughs 2 and 7, all of the troughs surveyed showed gas emissions.

Sedimentary strata were not visible in subbottom Parasound SLF profiles of the shallow shelf banks (Fig. 4b), but the troughs were characterized by reflections indicating sediment accumulations of up to ~40 m in their centers (Figs. 4a). The reflections were sub-parallel to the sea floor and presumably reflect accumulations of sediment transported from the fjords to the shelf, and deposition within the cross-shelf troughs. Numerous zones of acoustic blanking or acoustically-transparent chimneys that pierced the horizontal reflections were observed for all of the sediment infills within the troughs (Figs. 2b, 4a, b and c), which might be caused by upward gas migration at these sites. The acoustic chimneys were positioned directly underneath the acoustic flares in the water column in several areas, giving credence to the suggestion that the chimneys are the conduits for channeling free gas through the sediments towards the sea floor, where gas bubbles escape into the water column and form the flares imaged in the Parasound PHF echograms (Figs. 2b, 4a, b and c).

3.2 Visual sea floor observations at the 'Cumberland Bay Flare'

An OFOS deployment was conducted at a flare site designated as the 'Cumberland Bay Flare' in order to visually confirm the sea floor origin of the gas flares recorded hydroacoustically (Fig. 4c), and the nature of the surrounding sediments. The sea floor was inspected along an approx. 400 m long track (Fig. 5). The flat sea floor was composed of unconsolidated sediments and detached kelp fronds (Figs.

6a and b), many of which were partially buried. The observed epibenthic invertebrate megafauna included cidaroid and echinoid sea urchins, asteroid starfish, holothurians, hexactinellid sponges, and fish (Fig. 6a).

Numerous centimetre-sized holes were visible in the sea floor along the OFOS track, which were probably produced by endobenthic organisms or may represent the orifices of emanating gas bubbles. Rising gas bubbles were observed at two seep sites during the OFOS deployment, which was guided by flare observations in the water column. Our observations document gas bubbles emanating singly from the sea floor without forming continuous bubble streams. During an observation period of about 40 minutes at the southeastern located seep site (Figs. 5 and 6a), we documented more than 50 events (roughly about each minute), where a single bubble or pulses of 2 or 3 bubbles close together rose from the seabed. We observed individual rising gas bubbles again at a northwestern seep site, which is located ~50 m distant from the other and corresponded to a different water column flare (Figs. 5 and 6b).

At both seep sites the sea floor was covered by centimeter to decimeter-sized, subcircular, whitish material (Fig. 6a and b), occurring either as coherent patches or as collections of several smaller patches (Figs. 5 and 6a). These patches most probably represent microbial mats indicative of fluid flow from below. However, we did not see taxonomically higher chemosymbiotic organisms typically associated with cold seeps in other regions, such as bathymodiolin mussels or vesicomyid clams. The sea floor in two locations where whitish material was observed was elevated slightly and formed topographic mounds up to a few decimeters high (Fig. 6a). Fig. 5 illustrates that the whitish material was restricted to two areas a few meters in extent, both of which were located at the central foci of the two flares detected hydroacoustically.

3.3 Water column characteristics in Cumberland Bay

Three hydrocasts revealed a general water column stratification and specific differences in hydrological conditions in Cumberland Bay (station CTD-1 close to the ‘Cumberland Bay Flare’; CTD-2

close to the ‘Grytviken Flare’; see Fig. 3b) and a station seaward of the fjord (CTD-3; Fig. 7). A pronounced surface layer (upper ~20 mbsl) was present at stations CTD-1 and CTD-2 in Cumberland Bay, characterized by relatively low salinities (<33 PSU), temperatures (<2.8 °C) and beam transmissions (<80 %). These characteristics suggest that this water mass (not observed at the seaward station CTD-3; Figs. 7, supplementary Fig. S3) is affected by mixing with freshwater originating from the melting marine terminating glaciers (Fig. 3b). Physico-chemical properties varied only slightly with increasing depth throughout the midwater section. The lower limit of this water mass was found at ~165 mbsl for CTD-2 (located relatively deep within the fjord) and at ~190 mbsl for CTD-1 (located close to the fjord mouth), suggesting that its vertical extent is spatially variable and may reflect topographically-controlled circulation patterns. Similar water characteristics at all three investigated stations indicate water exchange between Cumberland Bay and the shelf area of South Georgia. The lowermost water mass within and outside Cumberland Bay was characterized by relatively low temperatures (~2.4 – 1.7°C) and relative depletions in dissolved oxygen concentrations (6.5 – 5.2 mL/l), but with the highest salinities (up to 34.2 PSU). A markedly lower beam transmission (as low as 80% at the bottom) recorded for the near-bottom water mass within the bay, if compared to that at the outer shelf station, might be the result of a higher particulate matter load (see also chapter 4.1).

Significant enrichments in dissolved methane of up to 25.4 nmol/l and 55.6 nmol/l, respectively, were measured in the lowermost water mass characterized by low-beam transmission at the two CTD stations taken in close proximity to the ‘Cumberland Bay Flare’ and the ‘Grytviken Flare’ (Figs. 3b and 7). At these stations concentrations of dissolved methane decreased significantly with decreasing depth within the lower 100-120 meters of the water column down to ca. 5 nmol/l (Fig. 7), which is still slightly elevated in contrast to the atmospheric equilibrium (3-3.3 nmol/l). At the outer shelf station, where flares were not detected, dissolved methane concentrations of <5 nmol/l were measured though the whole water column.

3.4 Stable carbon isotopic composition of methane

Stable carbon isotopic analysis of methane in the gas samples extracted from the two sediment cores taken in close proximity to flares (GC-1 within cross-shelf Trough 6; GC-2 in the Cumberland Bay; Figs. 3a and b) revealed strong depletions in ^{13}C, with $\delta^{13}C\text{-}CH_4$ values ranging between –80.2 and –88.9‰ (V-PDB). The greatest depletion came from a methane sample extracted at ~6.5 mbsf from the sediment core GC-2 at the 'Grytviken Flare'.

4. Discussion

4.1 Gas seeps at the northern shelf of South Georgia

We detected 133 gas flares at the northern shelf of South Georgia (Fig. 3a) during R/V Polarstern cruise ANT-XXIX/4 in 2013. Visual sea-floor inspections with the high-resolution video camera of the OFOS system confirmed active seepage at the 'Cumberland Bay Flare' in the form of rising gas bubbles and white sea-bed patches (Figs. 6a and b) interpreted as microbial mats fueled by methane emission. Hydroacoustically-imaged flares originated from sea floor locations that showed acoustically-blanked chimneys in the underlying sediments. In addition, water samples taken in bottom waters within two flares showed elevated concentrations of dissolved methane (Fig. 7), that proved methane transport by gas bubbles from the sea floor into the hydrosphere.

This new finding of methane seepage adds to the long and steadily growing list of seep areas in the world's oceans (Campbell, 2006; Judd and Hovland, 2007; Suess, 2010). At high latitudes, seeps are known in the Arctic and sub-Arctic, which have recently sparked particular scientific interest because of their links to permafrost settings (Shakhova et al., 2010) with potential global warming effects (Westbrook et al., 2009). Hydrothermal vents and cold seeps are known to host specialized faunal communities which are based on chemosynthesis (Bachraty et al., 2009; Van Dover et al., 2002). In the Southern Ocean to date only a few chemosynthetic ecosystems are known (Rogers and Linse, 2014), including the presently inactive cold seep in the western Weddell Sea, hydrothermal vent fields and a natural whale fall (Amon et al., 2013; Aquilina et al., 2013; Bohrmann et al., 1999;

Domack et al., 2005; Niemann et al., 2009; Rogers et al., 2012). The epibenthic invertebrate megafauna observed in the Cumberland Bay area comprises species commonly found around South Georgia (Hogg et al., 2011; James E. McKenna Jr., 1991; Jones et al., 2008). Except for the inferred microbial mats, chemosynthetic organisms usually found at cold seep sites were not found at the seeps investigated in this study. This might be because of the relatively shallow water depth (~250 mbsl), since the typical animals obligate at cold seeps (e.g. species of vesicomyid clams, bathymodiolin mussels and siboglinid tubeworms) are restricted to aphotic habitats. Explanations for their absence on the continental shelves include the abundance of predators in shallower waters, or competitive exclusion by primary consumers limiting the presence of species dependent on chemoautotrophic symbionts (Sahling et al., 2003). The exact depth limit is not precisely resolved (Little et al., 2002), but the shallowest seep communities with the typical obligate species found so far are reported from the Eel River basin, offshore California in ~350 mbsl (Orange et al., 2002) and in the Sea of Okhotsk in ~370 mbsl (Sahling et al., 2003). In our study we detected gas bubble seepage using hydroacoustics in the same depth range (ca. 380 mbsl), but did not investigate these sites visually. Thus, it remains a possibility that typical obligate cold seep animals are present on the deeper shelves around South Georgia.

As noted above, the flares detected during ANT-XXIX/4 along the northern shelf of South Georgia are not randomly distributed, but are restricted to the fjords and glacial troughs along the shelf (Fig. 3a), the latter accounting for ~15% of the total shelf area surrounding the island of South Georgia. A similar observation was made in a hydrocarbon seep area on the Baffin Bay shelf region, where oil and gas seeps were found within glacially-formed troughs seaward of fjord systems (Grant et al., 1986; Levy and Ehrhardt, 1981). In addition, seepage was inferred to occur in fjords in Spitsbergen (Forwick et al., 2009) and Norway (Judd and Hovland, 2007), based on the presence of sea floor pockmarks. Fjords generally appear to represent favorable settings for methane seepage as they are commonly characterized by high sedimentation rates due to high input from inflowing glaciers or meltwater streams. In addition, in some cases shallow water sills hamper water exchange with open

seawater areas and ventilation, favouring anoxic conditions and protecting organic material from rapid microbial decomposition under aerobic conditions, which finally leads to large accumulations of refractory organic matter in the sediments (Judd and Hovland, 2007). During our study we observed various sill structures in the high-resolution bathymetric maps of the South Georgia fjords, probably representing fjord moraines (Hodgson et al., 2014). However, these do not appear to fully restrict flow (Fig. 3b), as temperature, salinity and concentrations of dissolved oxygen are indeed lower in the bottom waters than in overlying water masses, but the values where similar in magnitude for all three stations, both within and outside the fjord. Therefore, there is no apparent isolation of the deep waters in Cumberland Bay (Figs. 7, supplementary Fig. S3). Bottom water oxygen concentrations within and outside the bay were ~5 mL/l (corresponding to ~220 µmol/l), indicating well-oxygenated conditions.

For Cumberland Bay, Platt (1979) estimated the sedimentation rate at 2.8×10^3 g m^{-2} yr^{-1} and an organic matter input of 60 g carbon m^{-2} yr^{-1}, providing an ideal setting for shallow biogenic methane production. A biogenic methane source is proven by $\delta^{13}C\text{-}CH_4$ values <–80 ‰ (V-PDB) for all gas samples collected from the two sediment cores we investigated. Methanogens preferentially consume substrates depleted in ^{13}C, whereas thermogenic light hydrocarbons by non-selective hydrocarbon cracking are not affected by significant isotope fractionation effects (Claypool and Kvenvolden, 1983). For a microbial hydrocarbon formation and accumulation both high sedimentation rate and the presence of sufficient amount of organic matter in the sediments are required. South Georgia lies in the eastward flowing Antarctic Circumpolar Current (ACC), creating a morphological high in the largest meander modifying the Southern ACC front (Meredith, 2003; Thorpe et al., 2002). Due to this particular hydrographic configuration, intensive and regular phytoplankton blooms develop in the area north and northwest of the South Georgia shelf (Borrione and Schlitzer, 2013), leading to both a rich food web (Atkinson et al., 2001), and a high carbon production, which is either exported (Schlitzer, 2002) or ultimately deposited at the sea floor. Although there is no indication for deeply buried reservoirs of thermogenic gas fueling the gas

emission sites investigated in this study, thermogenic hydrocarbon migration through deep-rooted faults cannot be entirely excluded as the fjords and connecting cross-shelf troughs may have established along lines of structural weakness that could have evolved in association to faults zones (Graham et al., 2008). Unfortunately, there are currently no seismic data imaging the deeper structure of the South Georgia block to test such a hypothesis. Lacking those data, we are also limited in discussion whether smaller geologic structures are controlling the seep distribution, such as those documented by Naudts et al. (2006) for the widespread seepage at the northwestern Black Sea margin. There, seeps were preferentially found in elongated pockmarks above margins of filled channels, along crests of sedimentary ridges, related to canyons or scarps of submarine landslides. In our study we discovered several flares rooted at morphological structures within the Cumberland Bay fjord, which were interpreted by Hodgson et al. (2014) as remnant or partially-preserved outer moraines and might support sub-surface channeling of migrating fluids. Other small-scale morphological features described by Hodgson et al. (2014), which include iceberg scours and pits or glacial debris, do not appear to be related to seepage.

4.2 Intensity of gas seepage and fate of methane in the water column

Most of the imaged flares during our surveys were not centered directly under the vessel, thus, precluding a quantitative assessment of their intensities. However, our observations revealed that (1) most flares are only few tens of meters high, (2) flares often appear episodically and are characterized by discharge in pulses, and (3) flares indicative for individual bubbles or bubble groups are occasionally tilted, so that their sea floor origin could not always be traced (Figs. 4a and b). These data suggest that most of the flares are rather weak and represent discontinuous releases of gas bubble emissions. Visual inspection of the 'Cumberland Bay Flare', one of the most intense flares we imaged (Fig. 4c), showed sporadic gas bubble discharge from the projected flare origin, but also indicated that the sporadic release of individual gas bubbles was sufficient to cause a relatively intense signature in the corresponding echogram. Our data demonstrate that the flares are temporally variable over minutes to weeks and it is likely that the activity and intensity of the gas

emissions may also change seasonally or annually. Due to the nature of our surveys, we are not able to resolve possible factors modulating the discharge (e.g. tides, earthquakes, storms events, bottom currents, decomposition of subsurface gas hydrates), as documented in more intensively investigated seep areas such as Hydrate Ridge (Kannberg et al., 2013), Coal Oil Point (Boles et al., 2001), Bush Hill (Solomon et al., 2008), or at seeps at the Northern Cascadia Margin (Lapham et al., 2013).

The quantity of bubbles and the intensity of seepage on the northern shelf of South Georgia seems to be rather weak in comparison to other seep areas, e.g. Hydrate Ridge (Heeschen et al., 2005; Torres et al., 2002), the Makran continental margin (Römer et al., 2012b), Santa Barbara channel (Hornafius, 1999), as well as several seepage areas in the Black Sea (Greinert et al., 2006; Naudts et al., 2006; Nikolovska et al., 2008; Pape et al., 2010; Römer et al., 2012a), where vigorous gas bubble emissions and/or strong flares have been documented. However, the large number of emission sites as revealed from our flare imaging, in combination with the significant enrichments in dissolved methane, suggests injection of non-negligible quantities of methane into the bottom water in fjords and the cross-shelf troughs of South Georgia, even though each individual seep may contribute only a small amount of methane. In addition, it is conceivable that our observations occurred in a period of minor seepage activity. For example, observations made for the Coal Oil Point seep field revealed interannual changes between 1990 and 2008, which have been related to internal geological processes (Bradley et al., 2010).

Our hydroacoustic data additionally indicate that most gas bubbles released into the water column probably did not reach the upper water layer and atmosphere, but instead dissolved entirely during their ascent. With three exceptions, all 133 flares detected disappeared from the SBES echograms well below the sea surface. Although the geometric limitation of the SBES coverage, particularly at shallow depths, has to be considered, the fraction of methane transported as gas bubbles is not limited only by the maximum bubble rising height, but mainly depends on the effectiveness of gas exchange processes taking place when entering the hydrosphere, due to concentration differences. The proportion of methane initially contained in the bubble is rapidly replaced by dissolved nitrogen

and oxygen from the ambient water (Leifer and Patro, 2002; McGinnis et al., 2006). The rapidity of this process strongly depends on the bubble size, the rise velocity, as well as the composition and conditions of the surrounding medium and the presence of upwelling flows (Leifer and Judd, 2002). Several studies have demonstrated that methane escapes the bubbles well before final bubble dissolution (Leifer and Patro, 2002; McGinnis et al., 2006; Rehder et al., 2002). Our suggestion that most of the methane discharged from the South Georgia northern shelf does not reach the upper water column is additionally strengthened by the relatively low concentrations of dissolved methane (about 5 nmol/l) in the intermediate to uppermost water masses at two hydrocast stations, deliberately acquired close to recorded flares in the Cumberland Bay area (Figs. 3b and 8). Most probably, the strong stratification of the water column, as evidenced by the T-S diagram (supplementary Fig. S3), impedes a regular vertical mixing within Cumberland Bay and the released methane therefore remains within the bottom water, leading to the observed profiles. A fraction of this methane may be oxidized through microbial activity (Reeburgh, 2007; Valentine et al., 2001), so the measured concentrations reflect a balance between methane input and bottom-water consumption within Cumberland Bay and water exchange with the outer shelf water. It is hard to directly correlate water column data with flare strength, but our data agree with our assumption that the methane transported via gas bubbles rapidly dissolves in the water body, so that most of the dissolved methane remains in the bottom water. Bubbles producing the hydroacoustic flares visible at that sites and reaching 50 m higher into the water column may have been depleted in methane.

5. Conclusion and Outlook

Hydroacoustic surveys and physico-chemical investigations of the water column in combination with visual sea floor inspections and analysis of sedimentary gas conducted on the northern shelf of South Georgia revealed the presence of widespread methane seepage from the sea floor into the water column. Flares occur restricted to the fjords and within glacial troughs along the shelf surrounding the island of South Georgia, which we confirmed has a biogenic source through isotopic analyses. This finding is to our knowledge the second cold seep detected in the (sub-)Antarctic region so far

and the first observation of a widespread and active area of seepage in the Southern Ocean. Detailed surveys are required to determine further distribution, variability, and total abundance of such methane seep sites, which is probably significantly higher than the 133 flares we detected during the detailed but still spatially-limited surveys of R/V Polarstern cruise ANT-XXIX/4.

We argue that the seepage around South Georgia is spatially related to the glacial trough and fjord system, a setting often occurring in sub-Antarctic regions that need further exploration to characterize the nature, distribution and magnitude of hydrocarbon seepage in this region. Because of the high organic matter input and presumed available methane reservoirs in the largely unexplored margins surrounding the Antarctic Peninsula (Murphy et al., 2013; Schlitzer, 2002; Wadham et al., 2012), and in the glacially-influenced shelves of various sub-Antarctic islands (Dickens et al., accepted), natural seepage in the Southern Ocean might be more common than previously thought.

Research questions arising from our methane seepage finding around South Georgia include: 1) unraveling the relationships between seepage, , rates of sediment accumulation, and the type and amount of organic carbon that sustain the methane reservoirs; 2) evaluating the potential contribution of thermogenic gas; 3) documenting the role of methane input on the biosphere and associated biogeochemical processes; 4) establishing whether some of the deeper seeps support chemosynthetic fauna, and, if present, determining whether they serve as 'stepping stones' for larval distribution of chemosynthesis-based organisms in the Southern Ocean; 5) constructing a carbon budget for the region, which includes source and consumption terms as well as the effect of circulation within and outside the fjords, and the circumstances under which this methane may reach the atmosphere.

6. Acknowledgements

We greatly appreciate the shipboard support from the master and crew of the research vessel Polarstern during cruise ANT-XXIX/4. This work was supported by the Deutsche

Forschungsgemeinschaft (DFG) in the framework of the priority program 'Antarctic Research with comparative investigations in Arctic ice areas' by a grant to BO 1049/19 and through the DFG-Research Center / Cluster of Excellence „The Ocean in the Earth System". AGCG was supported by Natural Environment Research Council (NERC) New Investigator Grant, NEK0005271, and by a fieldwork grant from the UK Quaternary Research Association (QRA) Research Fund. KL was supported by the ChEsSo programme (Consortium Grant NE/DO1249X/1) funded by NERC. CTSL acknowledges travel funds from the Earth Surface Sciences Institute, University of Leeds.

References

Amon, D.J., Glover, A.G., Wiklund, H., Marsh, L., Linse, K., Rogers, A.D., Copley, J.T., 2013. The discovery of a natural whale fall in the Antarctic deep sea. Deep-Sea Res.Pt II 92, 87–96.

Aquilina, A., Connelly, D.P., Copley, J.T., Green, D.R.H., Hawkes, J.A., Hepburn, L.E., Huvenne, V.A.I., Marsh, L., Mills, R.A., Tyler, P.A., 2013. Geochemical and Visual Indicators of Hydrothermal Fluid Flow through a Sediment-Hosted Volcanic Ridge in the Central Bransfield Basin (Antarctica). PLoS ONE 8.

Atkinson, A., Whitehouse, M., Priddle, J., Cripps, G., Ward, P., Brandon, M., 2001. South Georgia, Antarctica: a productive, cold water, pelagic ecosystem. Mar. Ecol.-Prog. Ser. 216, 279–308.

Bachraty, C., Legendre, P., Desbruyères, D., 2009. Biogeographic relationships among deep-sea hydrothermal vent faunas at global scale. Deep-Sea Res. Pt I 56, 1371–1378.

Barnes, R.O., Goldberg, E.D., 1976. Methane production and consumption in anoxic marine sediments. Geology, 4, 297-300.

Bohrmann, G., 2013. The expedition of the research vessel "Polarstern" to the Antarctic in 2013 (ANT-XXIX/4). Berichte zur Polar- und Meeresforschung = Reports on polar and marine research, Bremerhaven, Alfred Wegener Institute for Polar and Marine Research 668, 145 p.

Bohrmann, G., Chin, C., Petersen, S., 1999. Hydrothermal activity at Hook Ridge in the Central Bransfield Basin, Antarctica. Geo-Mar. Lett. 18, 277–284.

Boles, J.R., Clark, J.F., Leifer, I., Washburn, L., 2001.Temporal variation in natural methane seep rate due to tides, Coal Oil Point area, California. J. Geophys. Res, 106, 27077-27086.

Borrione, I., Schlitzer, R., 2013. Distribution and recurrence of phytoplankton blooms around South Georgia, Southern Ocean. Biogeosciences 10, 217–231.

Bradley E., Leifer, I., Roberts, D., 2010. Long-term monitoring of a marine geologic hydrocarbon source by a coastal air pollution station in Southern California, Atmos. Environ. 44, 4973-4981.

Campbell, K. A., 2006. Hydrocarbon seep and hydrothermal vent paleoenvironments and paleontology: Past developments and future research directions. Palaeogeogr. Palaeocl. 232, 362–407.

Caress, D.W., Clague, D.A., Paduan, J.B., Martin, J.F., Dreyer, B.M., Jr, W.W.C., Denny, A., Kelley, D.S., 2012. Repeat bathymetric surveys at 1-metre resolution of lava flows erupted at Axial Seamount in April 2011. Nat. Geosci. 5, 1–6.

Clark, J., Washburn, L., Schwager Emery, K., Variability of gas composition and flux intensity in natural marine hydrocarbon seeps, Geo-Mar. Lett. 30(2010) 379-388.

Claypool, G., Kvenvolden, K., 1983. Methane and other hydrocarbon gases in marine sediment. Annu. Rev. Earth Pl. Sc. 299–327.

Cunningham, a. P., Barker, P.F., Tomlinson, J.S., 1998. Tectonics and sedimentary environment of the North Scotia Ridge region revealed by side-scan sonar. J. Geol. Soc. London 155, 941–956.

Curtis, M.L., Flowerdew, M.J., Riley, T.R., Whitehouse, M.J., Daly, J.S., 2010. Andean sinistral transpression and kinematic partitioning in South Georgia. J. Struct.Geol. 32, 464–477.

Dalziel, I., Dott, R., 1975. Tectonic relations of South Georgia Island to the southernmost Andes. Bull. Geol. Soc. Am. 86, 1034–1040.

Davy, B., Pecher, I., Wood, R., Carter, L., Gohl, K., 2010.Gas escape features off New Zealand: Evidence of massive release of methane from hydrates. Geophys. Res. Lett., 37, L21309.

Dickens, W.A., Graham, A.G.C., Smith, J.A., Dowdeswell, J.A., Larter, R.D., Hillenbrand, C.-D., Trathan, P.N., Arndt, J.E., Kuhn, G., accepted. A new bathymetric compilation for the South Orkney Islands, Antarctic Peninsula (49°-39°W to 64°-59°S): insights into the glacial development of the continental shelf. doi: 10.1002/2014GC005323.

Domack, E., Ishman, S., Leventer, A., Sylva, S., Willmott, V., Huber, B., 2005. A chemotrophic ecosystem found beneath Antarctic Ice Shelf. Eos 86, 269.

Forsyth, D.W., 1975. Fault Plane Solutions and Tectonics of the South Atlantic and Scotia Sea. J. Geophys. Res. 80, 1429-1443.

Forwick, M., Baeten, N.J., Vorren, T.O., 2009. Pockmarks in Spitsbergen fjords. Norw. J. Geol. 89, 65–77.

Fretwell, P.T., Tate, a. J., Deen, T.J., Belchier, M., 2008. Compilation of a new bathymetric dataset of South Georgia. Antarct. Sci. 21, 171.

Gentz, T., Damm, E., Schneider von Deimling, J., Mau, S., McGinnis, D.F., Schlüter, M., 2013. A water column study of methane around gas flares located at the West Spitsbergen continental margin. Cont. Shelf Res. 1–12.

Graham, A.G.C., Fretwell, P.T., Larter, R.D., Hodgson, D. a., Wilson, C.K., Tate, A.J., Morris, P., 2008. A new bathymetric compilation highlighting extensive paleo-ice sheet drainage on the continental shelf, South Georgia, sub-Antarctica. Geochem. Geophy. Geosy. 9, Q07011.

Grant, A., Levy, E., Lee, K., Moffat, J., 1986. Pisces lV research submersible finds oil on Baffin Shelf. Current Research, Part A, Geological Survey of Canada 86, 65–59.

Greinert, J., Artemov, Y., Egorov, V., Debatist, M., Mcginnis, D., 2006. 1300-m-high rising bubbles from mud volcanoes at 2080m in the Black Sea: Hydroacoustic characteristics and temporal variability. Earth Planet. Sc. Lett. 244, 1–15.

Greinert, J., McGinnis, D.F., 2009. Single bubble dissolution model – The graphical user interface SiBu-GUI. Environ. Modell. Softw. 24, 1012–1013.

Greinert, J., McGinnis, D.F., Naudts, L., Linke, P., De Batist, M., 2010. Atmospheric methane flux from bubbling seeps: Spatially extrapolated quantification from a Black Sea shelf area. J. Geophys.Res. 115, C01002.

Griffiths, H.J., 2010. Antarctic marine biodiversity-what do we know about the distribution of life in the Southern Ocean? PloS one 5(8): e11683. doi:10.1371/journal.pone.0011683.

Hanson, R.S., Hanson, T.E., 1996. Methanotrophic bacteria. Microbiological Reviews, 60, 439-471.

Heeschen, K.U., Collier, R.W., de Angelis, M. a., Suess, E., Rehder, G., Linke, P., Klinkhammer, G.P., 2005. Methane sources, distributions, and fluxes from cold vent sites at Hydrate Ridge, Cascadia Margin. Global Biogeochem. Cy. 19, GB2016.

Hinrichs, K., Boetius, A., 2002. The anaerobic oxidation of methane: new insights in microbial ecology and biogeochemistry, in: Wefer, G., Billett, D., Hebbeln, D., Jørgensen, B.B., Schlüter, M., (Ed.), Ocean Margin Systems. Springer-Verlag Berlin Heidelberg, pp. 457–477.

Hodgson, D.A., Graham, A.G.C., Griffiths, H.J., Roberts, S.J., Cofaigh, C.Ó., Bentley, M.J., Evans, D.J., 2014. Glacial history of sub-Antarctic South Georgia based on the submarine geomorphology of its fjords. Quaternary Sci.Rev., 89, 129-147.

Hogg, O.T., Barnes, D.K.A., Griffiths, H.J., 2011. Highly Diverse , Poorly Studied and Uniquely Threatened by Climate Change : An Assessment of Marine Biodiversity on South Georgia's Continental Shelf. PLoS ONE 6.

Hornafius, J., 1999. The world's most spectacular marine hydrocarbon seeps (Coal Oil Point, Santa Barbara Channel, California): Quantification of emissions. J. Geophys. Res. 104, 20,703 – 20,711.

Hyndman, R.D., Davis, E.E., 1992. A mechanism for the formation of methane hydrate and seafloor bottom-simulating reflectors by vertical fluid expulsion. Journal of Geophysical Research: Solid Earth, 97, 7025-7041.

Intergovernmental Panel on Climate Change (IPCC), 2007: Climate Change 2007, Cambridge University Press, Cambridge, United Kingdom and New York, USA, 996 pp.

James E. McKenna Jr., 1991. Trophic Relationships within the Antarctic Demersal Fish Community of South Georgia Island. Fish. B.-NOAA 89, 643–654.

Jones, C.D., Anderson, M.E., Balushkin, A. V, Duhamel, G., Eakin, R.R., Eastman, J.T., Kuhn, K.L., Lecointre, G., Near, T.J., North, A.W., Stein, D.L., Vacchi, M., Detrich, H.W., 2008. Diversity, relative abundance, new locality records and population structure of Antarctic demersal fishes from the northern Scotia Arc islands and Bouvetøya. Polar Biol. 31, 1481–1497.

Jones, E.M., Bakker, D.C.E., Venables, H.J., Watson, A.J., 2012. Dynamic seasonal cycling of inorganic carbon downstream of South Georgia, Southern Ocean. Deep-Sea Res. Pt II 59-60, 25–35.

Judd, A.G., Hovland, M., 1992.The evidence of shallow gas in marine sediments. Cont. Shelf Res., 12, 1081-1095.

Judd, A.G., Hovland, M., 2007. Seabed fluid flow. Cambridge University Press.

Kannberg, P.K., Tréhu, A.M., Pierce, S.D., Paull, C.K., Caress, D.W., 2013. Temporal variation of methane flares in the ocean above Hydrate Ridge, Oregon. Earth Planet. Sci. Lett., 368, 33-42.

Knittel, K., Boetius, A., 2009.Anaerobic oxidation of methane: Progress with unknown process. Annu. Rev. Microbiol., 63, 311-334.

Lapham, L., Wilson, R., Riedel, M., Paull, C.K., Holmes, M.E., 2013.Temporal variability of in situ methane concentrations in gas hydrate-bearing sediments near Bullseye Vent, Northern Cascadia margin. Geochem. Geophys. Geosyst., 14(7), doi: 10.1002/ggg.20167.

Leifer, I., Judd, A.G., 2002. Oceanic methane layers: the hydrocarbon seep bubble deposition hypothesis. Terra Nova 14, 417–424.

Leifer, I., Patro, R.K., 2002. The bubble mechanism for methane transport from the shallow sea bed to the surface: A review and sensitivity study. Cont.Shelf Res. 22, 2409–2428.

Levy, E., Ehrhardt, M., 1981. Natural seepage of petroleum at Buchan Gulf, Baffin Island. Mar. Chem. 10, 355–364.

Little, C., Campbell, K., Herrington, R., 2002. Why did ancient chemosynthetic seep and vent assemblages occur in shallower water than they do today? Comment. Int. J. Earth Sci. 91, 149–153.

Logan, G.A., Jones, A.T., Kennard, J.M., Ryan, G.J., Rollet, N., 2010. Australian offshore natural hydrocarbon seepage studies, a review and re-evaluation. Mar. Pet. Geol., 27, 26-45.

Ludwig, W.J., Rabinowitz, P.D., 1982. The collision complex of the North Scotia Ridge. J. Geophys. Res. 87, 3731.

MacDonald, D.I.M., Storey, B.C., 1987. South Georgia, BAS GEOMAP Series, Sheet 1, scale 1:250,000. British Antarctic Survey, Cambridge, U. K.

Mau, S., Heintz, M.B., Valentine, D.L., 2012. Quantification of CH4 loss and transport in dissolved plumes of the Santa Barbara Channel, California. Cont. Shelf Res. 32, 110–120.

McGinnis, D.F., Greinert, J., Artemov, Y., Beaubien, S.E., Wüest, a., 2006. Fate of rising methane bubbles in stratified waters: How much methane reaches the atmosphere? J. Geophys. Res. 111, C09007.

Meredith, M.P., 2003. An anticyclonic circulation above the Northwest Georgia Rise, Southern Ocean. Geophys. Res. Lett. 30, 2061.

Meredith, M.P., Brandon, M. a., Murphy, E.J., Trathan, P.N., Thorpe, S.E., Bone, D.G., Chernyshkov, P.P., Sushin, V. a., 2005. Variability in hydrographic conditions to the east and northwest of South Georgia, 1996–2001. J. Marine Syst. 53, 143–167.

Murphy, E. J., Hofmann, E. E., Watkins, J. L., Johnston, N. M., Piñones, A., Ballerini, T., Hill, S.L. , Trathan, P.N., Tarling, G.A., Cavanagh, R.A. , Young, E.F., Thorpe, S.E., Fretwell, P. ,2013. Comparison of the structure and function of Southern Ocean regional ecosystems: The Antarctic Peninsula and South Georgia. Journal of Marine Systems, 109-110, 22–42.

Murrell, J.C., 2010. The Aerobic Methane Oxidizing Bacteria (Methanotrophs), in: Timmis, K.N. (Ed.), Handbook of Hydrocarbon and Lipid Microbiology. Springer Berlin Heidelberg, Berlin, Heidelberg, pp. 1953–1966.

Naudts, L., Greinert, J., Artemov, Y., Staelens, P., Poort, J., Van Rensbergen, P., De Batist,M., 2006. Geological and morphological setting of 2778 methane seeps in the Dnepr paleo-delta, northwestern Black Sea, Mar. Geol., 227, 177-199.

Niemann, H., Fischer, D., Graffe, D., Knittel, K., Montiel, a., Heilmayer, O., Nöthen, K., Pape, T., Kasten, S., Bohrmann, G., Boetius, a., Gutt, J., 2009. Biogeochemistry of a low-activity cold seep in the Larsen B area, western Weddell Sea, Antarctica. Biogeosciences 6, 2383–2395.

Nikolovska, A., Sahling, H., Bohrmann, G., 2008. Hydroacoustic methodology for detection, localization, and quantification of gas bubbles rising from the seafloor at gas seeps from the eastern Black Sea. Geochem. Geophy. Geosy. 9, Q10010.

Orange, D.L., Yun, J., Maher, N., Barry, J., Greene, G., 2002. Tracking California seafloor seeps with bathymetry, backscatter and ROVs. Cont. Shelf Res. 22, 2273–2290.

Pape, T., Bahr, A., Rethemeyer, J., Kessler, J.D., Sahling, H., Hinrichs, K.-U., Klapp, S.A., Reeburgh, W.S., Bohrmann, G., 2010. Molecular and isotopic partitioning of low-molecular-weight hydrocarbons during migration and gas hydrate precipitation in deposits of a high-flux seepage site. Chem. Geol. 269, 350–363.

Pape, T., P. Geprägs, S. Hammerschmidt, P. Wintersteller, J. Wei, T. Fleischmann, G. Bohrmann, A. J. Kopf, 2014. Hydrocarbon seepage and its sources at mud volcanoes of the Kumano forearc basin, Nankai Trough subduction zone, Geochemistry, Geophysics, Geosystems, n/a-n/a, 10.1002/2013gc005057.

Pelayo, A., Wiens, D., 1989. Seismotectonics and relative plate motions in the Scotia Sea region. J. Geophys.Res. 94, 7293–7320.

Platt, H.M., 1979. Sedimentation and the distribution of organic matter in a sub-Antarctic marine bay. Estuar. Coast. Mar. Sci. 9, 51–63.

Reeburgh, W.S., 2007.Oceanic methane biogeochemistry. Chem. Rev., 107, 486-513.

Rehder, G., Keir, R.S., Suess, E., Rhein, M., 1999. Methane in the northern Atlantic controlled by microbial oxidation and atmospheric history. Geophysical Research Letters 26, 587–590.

Rehder, G., Brewer, P.W., Peltzer, E.T., Friederich, G., 2002. Enhanced lifetime of methane bubble streams within the deep ocean, Geophys. Res. Lett. 29, 1731-1734.

Rogers, A.D., Linse, K., 2014. Chemosynthetic communities, in: De Broyer C., Koubbi P., Griffiths H., Danis B., D.B. et al. (Ed.), Biogeographic Atlas of the Southern Ocean. Scientific Committee on Antarctic Research, Cambridge, pp. 2–6.

Rogers, A.D., Tyler, P.A, Connelly, D.P., Copley, J.T., James, R., Larter, R.D., Linse, K., Mills, R.A, Garabato, A.N., Pancost, R.D., Pearce, D. a, Polunin, N.V.C., German, C.R., Shank, T., Boersch-Supan, P.H., Alker, B.J., Aquilina, A., Bennett, S.A, Clarke, A., Dinley, R.J.J., Graham, A.G.C., Green, D.R.H., Hawkes, J., Hepburn, L., Hilario, A., Huvenne, V., Marsh, L., Ramirez-Llodra, E., Reid, W.D.K., Roterman, C.N., Sweeting, C.J., Thatje, S., Zwirglmaier, K., 2012. The discovery of new deep-sea hydrothermal vent communities in the southern ocean and implications for biogeography. PLoS Biology 10, e1001234.

Römer, M., Sahling, H., Pape, T., Bahr, A., Feseker, T., Wintersteller, P., Bohrmann, G., 2012a. Geological control and magnitude of methane ebullition from a high-flux seep area in the Black Sea-the Kerch seep area. Mar. Geol. 319-322, 57–74.

Römer, M., Sahling, H., Pape, T., Bohrmann, G., Spieß, V., 2012b. Quantification of gas bubble emissions from submarine hydrocarbon seeps at the Makran continental margin (offshore Pakistan). J. Geophys. Res. 117, C10015.

Sahling, H., Galkin, S. V, Salyuk, A., Greinert, J., Foerstel, H., Piepenburg, D., Suess, E., 2003. Depth-related structure and ecological significance of cold-seep communities—a case study from the Sea of Okhotsk. Deep-Sea Res. Pt I 50, 1391–1409.

Schlitzer, R., 2002. Carbon export fluxes in the Southern Ocean: results from inverse modeling and comparison with satellite-based estimates. Deep-Sea Res. Pt II 49, 1623–1644.

Sellanes, J., Quiroga, E., Gallardo, V. A., 2004. First direct evidence of methane seepage and associated chemosynthetic communities in the bathyal zone off Chile. J. Mar. Biol. Assoc. U.K., 84, 1065-1066.

Shakhova, N., Semiletov, I., Salyuk, A., Yusupov, V., Kosmach, D., Gustafsson, O., 2010. Extensive methane venting to the atmosphere from sediments of the East Siberian Arctic Shelf. Science 327, 1246–50.

Shakhova, N. Semiletov, I., Leifer, I., Sergienko, V., Salyuk, A., Kosmach, D., Chernykh, D., Stubbs, C., Nicolsky, D., Tumskoy, V., Gustafsson, O., Ebullition and storm-induced methane release from the East Siberian Arctic Shelf, Nature Geosci 7(2014) 64-70.Simpson, P., Griffiths, D.H., 1982. The structure of the South Georgia Continental Block, in: Craddock, C. (Ed.), Antarctic Geoscience, IUGS Ser. B, Vol. 4. Int. Union of Geol. Sci., Trondheim, Norway, pp. 185 – 191.

Solomon, E.A., Kastner, M., Jannasch, H., Robertson, G., Weinstein, Y., 2008.Dynamic fluid flow and chemical fluxes associated with a seafloor gas hydrate deposit on the northern Gulf of Mexico slope. Earth Planet. Sci. Lett., 270, 95-105.

Suess, E., 2010. Transfer from the Geosphere to Biosphere: 12 Marine Cold Seeps, in: Timmis, K.N. (Ed.), Handbook of Hydrocarbon and Lipid Microbiology. pp. 186–203.

Thorpe, S.E., Heywood, K.J., Brandon, M.A, Stevens, D.P., 2002. Variability of the southern Antarctic Circumpolar Current front north of South Georgia. J. Marine Syst. 37, 87–105.

Torres, M.E., Mcmanus, J., Hammond, D.E., Angelis, M.A. De, Heeschen, K.U., Colbert, S.L., Tryon, M.D., Brown, K.M., Suess, E., 2002. Fluid and chemical fuxes in and out of sediments hosting methane hydrate deposits on Hydrate Ridge , OR , I : Hydrological provincesEarth Planet. Sc. Lett. 201, 525–540.

Valentine, D., Blanton, D., Reeburgh, W.S., Kastner, M., 2001. Water column methane oxidation adjacent to an area of active hydrate dissociation, Eel River Basin. Geochim. Cosmochim. Ac. 65, 2633–2640.

Van Dover, C.L., German, C.R., Speer, K.G., Parson, L.M., Vrijenhoek, R.C., 2002. Evolution and biogeography of deep-sea vent and seep invertebrates. Science 295, 1253–7.

Wadham, J.L., Arndt, S., Tulaczyk, S., Stibal, M., Tranter, M., Telling, J., Lis, G.P., Lawson, E., Ridgwell, A., Dubnick, A., Sharp, M.J., Anesio, A. M., Butler, C.E.H., 2012. Potential methane reservoirs beneath Antarctica. Nature 488, 633–7.

Westbrook, G.K., Thatcher, K.E., Rohling, E.J., Piotrowski, A.M., Pälike, H., Osborne, A.H., Nisbet, E.G., Minshull, T. a., Lanoisellé, M., James, R.H., Hühnerbach, V., Green, D., Fisher, R.E., Crocker, A.J., Chabert, A., Bolton, C., Beszczynska-Möller, A., Berndt, C., Aquilina, A., 2009. Escape of methane gas from the seabed along the West Spitsbergen continental margin. Geophys. Res. Lett. 36, L16608.

Whiticar, M.J., 1999. Carbon and hydrogen isotope systematics of bacterial formation and oxidation of methane. Chem. Geol. 161, 291-314.

Young, E.F., Meredith, M.P., Murphy, E.J., Carvalho, G.R., 2011. High-resolution modelling of the shelf and open ocean adjacent to South Georgia, Southern Ocean. Deep-Sea Res.Pt II 58, 1540–1552.

Figure captions

Fig. 1 a) Plate tectonic overview with the South Georgia microplate (SG) located at the eastern part of the North Scotia Ridge. SAM: South American Plate, SCO: Scotia Plate, SAN: Sandwich Plate, ANT: Antarctic Plate (modified after Cunningham et al., 1998). b) Map of the main tectonic structures of the South Georgia crustal block (after MacDonald and Storey, 1987). The shelf morphology is characterized by at least ten cross-shelf troughs sourcing at the fjords of the island (yellow areas; Graham et al., 2008).

Fig. 2 a) Echogram recorded with the single beam echosounder (SBES) illustrating a flare composed of numerous oblique high-backscatter traces representing uprising gas bubbles. The footprint of the SBES at a water depth of ~380 mbsl corresponds to ~30 m width of the flare signal at the sea floor (white line). b) SBES echogram combing the water column data and the subbottom information

(using 18 and 3.5 kHz frequencies, respectively). Gas emission sites are characterized by acoustic blanking in the subsurface (gas chimneys) and emissions of free gas in the water column causing hydroacoustic flares. For locations see Figs. 3a and b.

Fig. 3 a) Shelf bathymetry with its characteristic cross-shelf troughs in combination with the ship track (black line) and flare positions (red dots) detected during R/V Polarstern cruise ANT-XXIX/4. Cross-shelf Troughs 1-7 at the northern shelf have been crossed in order to detect free gas in the subbottom and water column. Additionally, two fjords were investigated: the Possession Bay, where Trough 4 is sourced, and the Cumberland Bay, which is directly connected to Trough 5. b) Detailed map of the Cumberland Bay with the processed bathymetric data acquired during cruise ANT-XXIX/4. More than 75 flares were detected during the surveys within the fjord system.

Fig. 4 Three profiles recorded with SBES combining subbottom (3.5 kHz) and water column (18 kHz) information. Flares are repainted in red. For locations see Figs. 3a and b. a) Profile 1 shows an echogram crossing the cross-shelf Trough 4. Several flares were detected with the majority showing a discontinuous pattern most probably caused by pulsing gas bubble emissions. b) Profile 2 shows an echogram at cross-shelf Trough 6. In contrast to the shallow banks lacking visible sediment strata in the subbottom, the troughs are characterized by sediment accumulation. c) Profile 3 shows an echogram recorded during entering of the Cumberland Bay and crossing the 'Cumberland Bay flare'. Several acoustic chimneys characterized by vertical blanking zones illustrate rising free gas in the subbottom (red outlines with arrows) and three flares demonstrating the emission of gas bubbles into the water column.

Fig. 5 a) Bathymetric map from ship-based swath echosounder recordings with the dive track of the Ocean Floor Observation System (OFOS; station PS81/285-1) passing two areas, where hydroacoustic investigations indicated gas bubble emissions from the sea floor (light red circles). Rising gas bubbles were recognized in both areas and whitish patches on the sea floor additionally suggested the position of the seep sites (white dots).

Fig. 6 a) Sea floor picture taken at the Cumberland Bay Flare with the high-resolution video camera mounted on the frame of the Ocean Floor Observation System (OFOS) and showing an elongated mounded structure at the sea floor characterized by whitish color, probably representing microbial mats. b) Sea floor image taken at the northwestern flare area demonstrates the occurrence and intercalation of white colored and additionally dark grey colored patches. For locations see Figs. 3b and 5.

Fig. 7 Water column profile illustrating selected data recorded during three CTD casts. Stations CTD-1 (colored dashed lines) and CTD-2 (colored solid lines) were located within the Cumberland Bay and CTD-3 (black lines) seaward the fjord mouth (see Fig. 3b). Elevated methane concentrations were measured in particular in the lowermost ~100 m at the two Cumberland Bay stations taken close to hydroacoustically detected flares. Bottom waters at that depth were characterized by low temperatures, beam transmissions and dissolved oxygen concentrations.

Supplementary Fig. S3 Temperature-Salinity diagram of the data from the three CTD stations during ANT-XXIX/4. T-S condition in surface waters at stations CTD-1 and CTD-2 located in the Cumberland Bay clearly differed from those at station CTD-3 positioned seaward (for locations see Fig. 3b).

775 Fig. 1

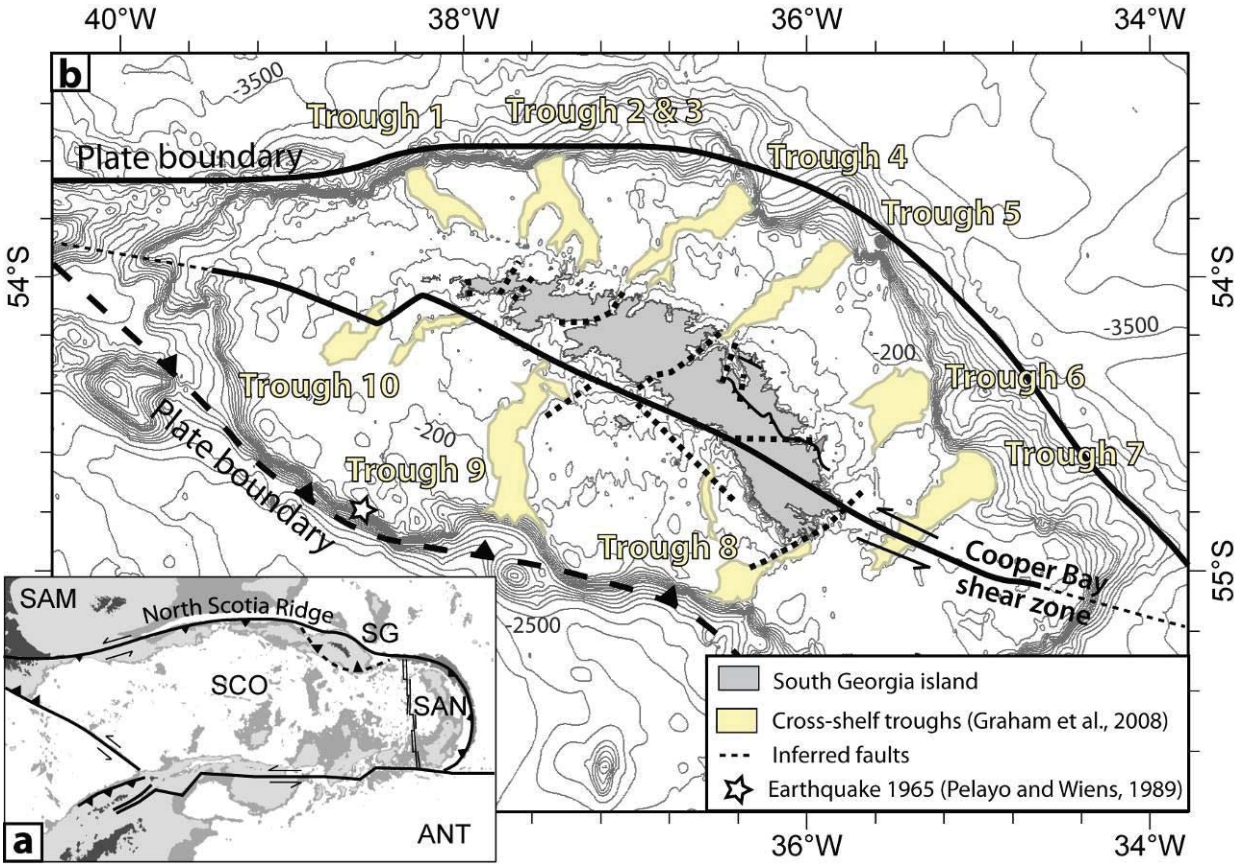
40°W
38°W
36°W
34°W
54°S
55°S
b
-3500
Trough 1
Trough 2 & 3
Plate boundary
Trough 4
Trough 5
-3500
-200
Trough 6
Trough 10
-200
Trough 9
Trough 7
Plate boundary
Trough 8
Cooper Bay
shear zone
-2500
South Georgia island
Cross-shelf troughs (Graham et al., 2008)
Inferred faults
Earthquake 1965 (Pelayo and Wiens, 1989)
SAM
North Scotia Ridge
SG
SCO
SAN
ANT
a

Fig. 2

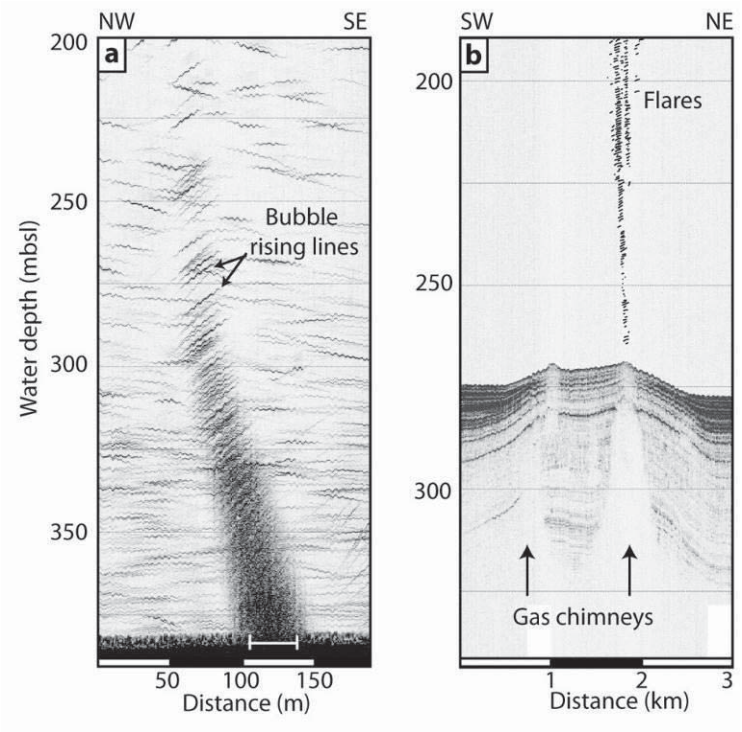
NW
SE
a
200
250
300
350
Water depth (mbsl)
Bubble
rising lines
50
100
150
Distance (m)
SW
NE
b
200
250
300
Flares
Gas chimneys
1
2
3
Distance (km)

780 Fig. 3

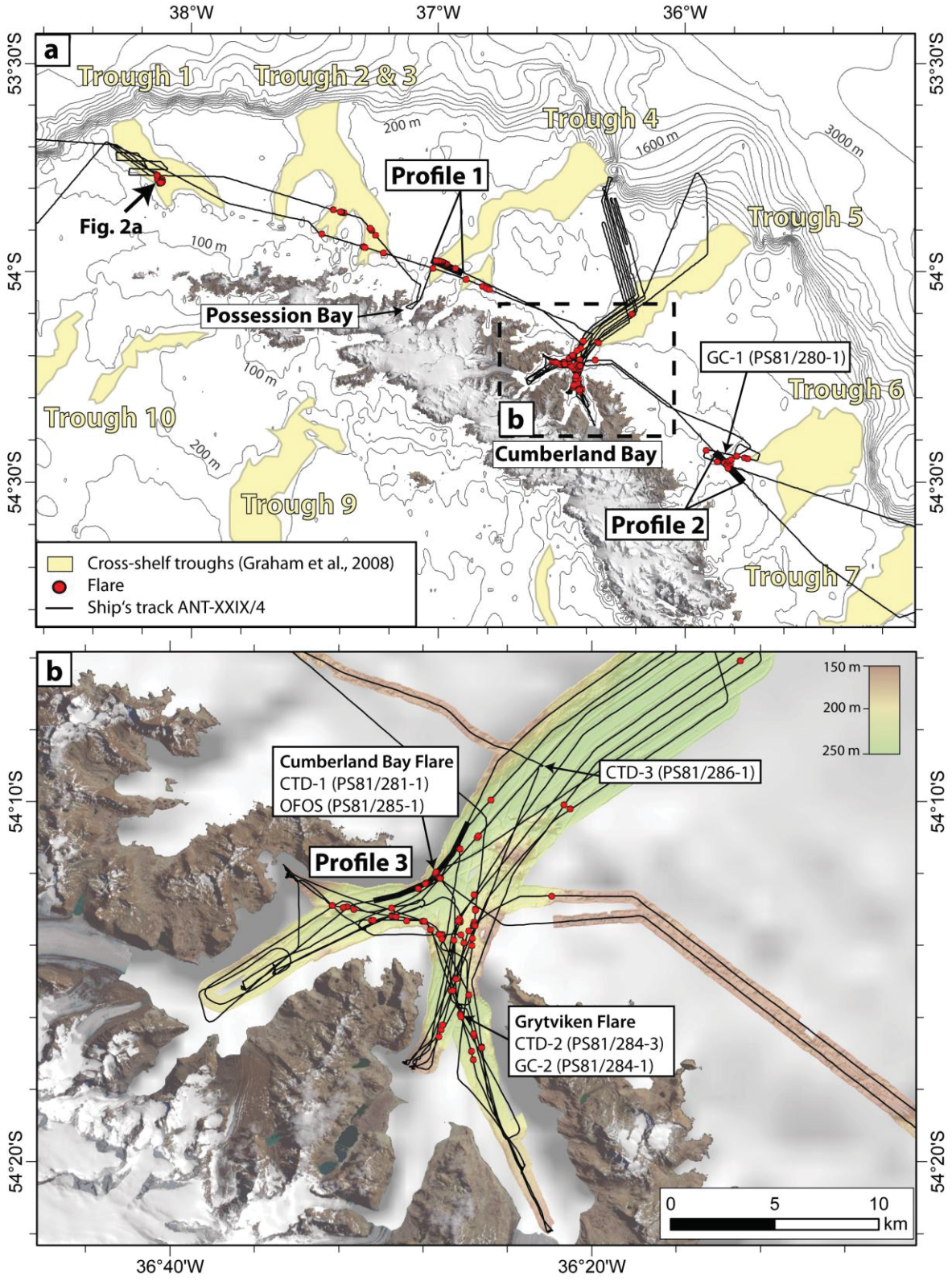
a
Trough 1
Trough 2 & 3
Trough 4
Trough 5
Trough 6
Trough 7
Trough 9
Trough 10
200 m
1600 m
3000 m
100 m
100 m
200 m
Profile 1
Fig. 2a
Possession Bay
GC-1 (PS81/280-1)
b
Cumberland Bay
Profile 2
Cross-shelf troughs (Graham et al., 2008)
Flare
Ship's track ANT-XXIX/4
38°W
37°W
36°W
53°30'S
54°S
54°30'S
b
150 m
200 m
250 m
Cumberland Bay Flare
CTD-1 (PS81/281-1)
OFOS (PS81/285-1)
CTD-3 (PS81/286-1)
Profile 3
Grytviken Flare
CTD-2 (PS81/284-3)
GC-2 (PS81/284-1)
0
5
10
km
54°10'S
54°20'S
36°40'W
36°20'W

Fig. 4

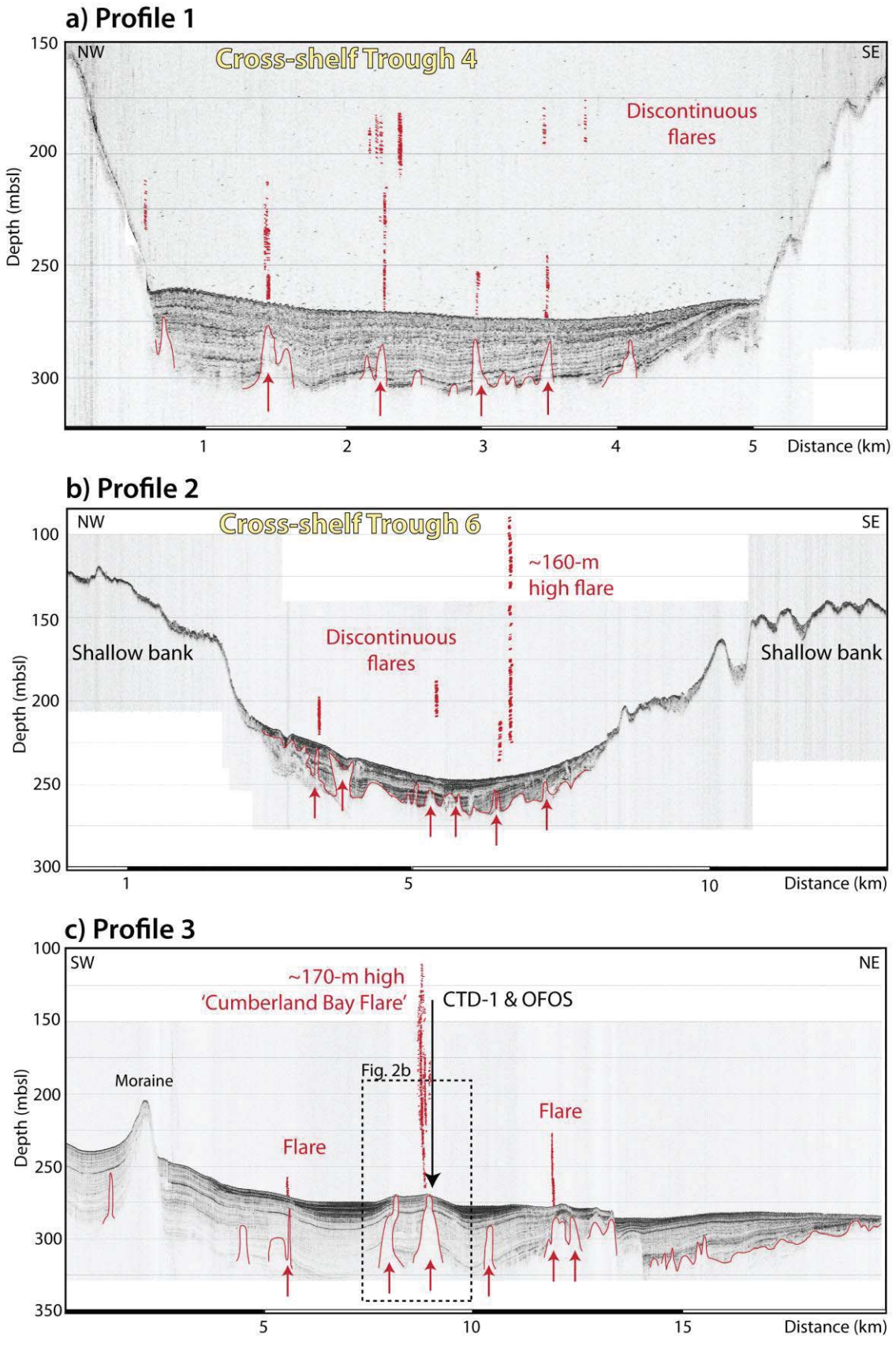
a) Profile 1
NW
SE
Cross-shelf Trough 4
Discontinuous flares
Depth (mbsl)
150
200
250
300
1
2
3
4
5
Distance (km)
b) Profile 2
NW
SE
Cross-shelf Trough 6
~160-m high flare
Discontinuous flares
Shallow bank
Shallow bank
Depth (mbsl)
100
150
200
250
300
1
5
10
Distance (km)
c) Profile 3
SW
NE
~170-m high 'Cumberland Bay Flare'
CTD-1 & OFOS
Fig. 2b
Moraine
Flare
Flare
Depth (mbsl)
100
150
200
250
300
350
5
10
15
Distance (km)

785

Fig. 5

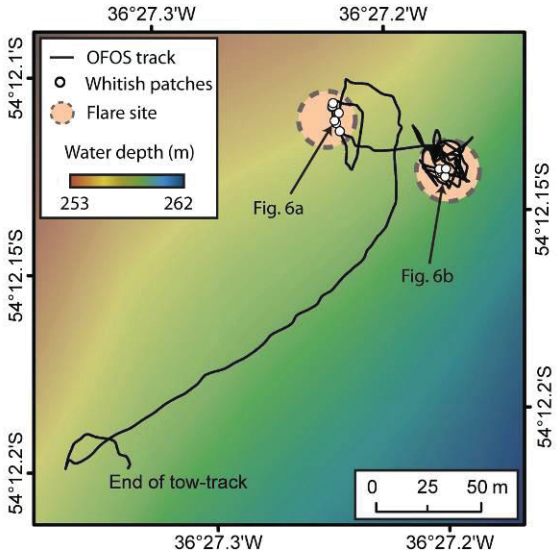
36°27.3'W
36°27.2'W
54°12.1'S
54°12.15'S
54°12.2'S
OFOS track
Whitish patches
Flare site
Water depth (m)
253
262
Fig. 6a
Fig. 6b
End of tow-track
0
25
50 m

790

Fig. 6

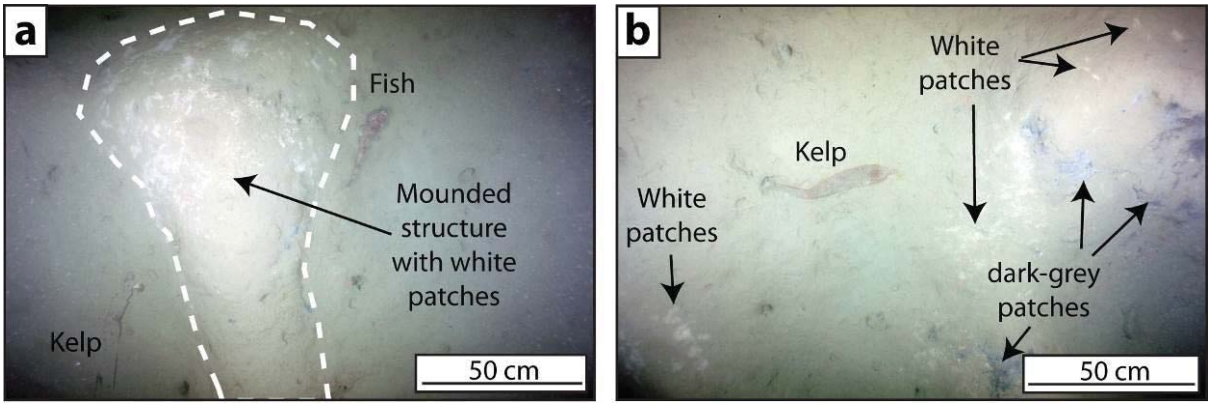
a
Fish
Mounded structure with white patches
Kelp
50 cm
b
White patches
Kelp
White patches
dark-grey patches
50 cm

Fig. 7

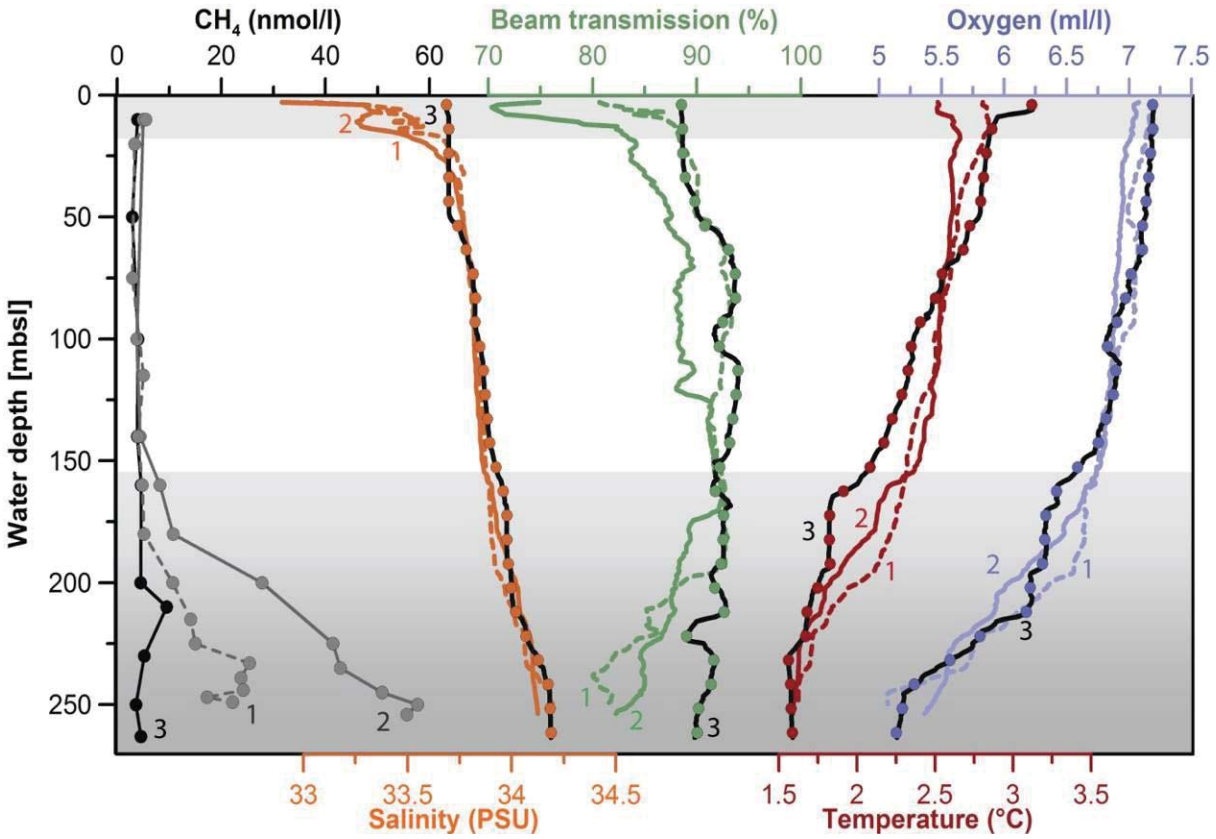
CH4 (nmol/l)
Beam transmission (%)
Oxygen (ml/l)
Water depth [mbsl]
Salinity (PSU)
Temperature (°C)

795